ELSEVIER

Chemistry & Biology 8 (2001) 1051–1060

Chemistry & Biology

www.elsevier.com/locate/chembiol

Research Paper

A novel fluorescent silica tracer for biological silicification studies

Katsuhiko Shimizu [a,d,e,1], Yolanda Del Amo [b,d,e,2], Mark A. Brzezinski [b,d,e], Galen D. Stucky [c,e], Daniel E. Morse [a,d,e,*]

[a] *Department of Molecular, Cellular and Developmental Biology, University of California, Santa Barbara, CA 93106 USA*
[b] *Department of Ecology, Evolution and Marine Biology, University of California, Santa Barbara, CA 93106 USA*
[c] *Departments of Chemistry and Materials, University of California, Santa Barbara, CA 93106 USA*
[d] *Marine Science Institute, University of California, Santa Barbara, CA 93106 USA*
[e] *Materials Research Laboratory, University of California, Santa Barbara, CA 93106 USA*

Received 15 May 2001; revisions requested 6 July 2001; revisions received 16 July 2001; accepted 20 July 2001
First published online 12 September 2001

Abstract

Background: Biological silica production has drawn intense attention and several molecules involved in biosilicification have been identified. Cellular mechanisms, however, remain unknown mainly due to the lack of probes required for obtaining information on live specimens.

Results: The fluorescence spectra of the compound 2-(4-pyridyl)-5-((4-(2-dimethylaminoethylaminocarbamoyl)methoxy)-phenyl)oxazole (PDMPO) are affected by the presence of >3.2 mM silicic acid. Increase in intensity and shift in the fluorescence coincide with the polymerization of Si. The unique PDMPO–silica fluorescence is explored here to visualize Si deposition in living diatoms. The fluorophore is selectively incorporated and co-deposited with Si into the newly synthesized frustules (the outer silica shells) showing an intense green fluorescence.

Conclusions: We suggest that a fluorescence shift is due to an interaction between PDMPO and polymeric silicic acid. PDMPO is an excellent probe for imaging newly deposited silica in living cells and has also a potential for a wide range of applications in various Si-related disciplines, including biology of living organisms as diatoms, sponges, and higher plants, clinical research (e.g. lung fibrosis and cancer, bone development, artificial bone implantation), and chemistry and physics of materials research.

Keywords: Biomineralization; Diatom; Fluorescence; pH indicator; Silica

1. Introduction

Silicon (Si), the second most abundant element of the earth's crust, is a highly valued element due to the wide range of industrially produced silica-based materials, such as zeolites and other porous materials. However, chemical synthesis of many useful silica-based materials requires extreme conditions of temperature, pressure and pH, as well as non-aqueous solvents, and highly ordered structures are still challenging to obtain.

In nature, Si is also an essential element both in plant and animal life, including diatoms, sponges, mollusks and higher plants [1]. Diatoms are microalgae that take up dissolved Si from the water (fresh- or seawater) to produce silicified cell walls containing amorphous silica (frustules) with highly detailed species-specific morphological features. The remains of these frustules preserved in ancient seabeds comprise the diatomite or diatomaceous earth mined from uplifted marine deposits on land. The wide range of industrial applications of diatomite (such as fillers, catalysts, insulators, molecular sieves or filters, abrasives and absorbents) is due to its uniformity in particle size, its highly ordered structure and of course, its large availability. Due to the remarkable and diversified structures of these 'biosystems', the search for new 'bioinspired' high performance composite materials has recently drawn extensive attention to the mechanisms involved in biolog-

[1] Present address: Department of Histology and Neurobiology, School of Medicine, Dokkyo University, Mibu, Tochigi, 321-0297 Japan.

[2] Present address: Laboratoire d'Océanographie Biologique, UMR CNRS 5805 - Université Bordeaux 1, Station Marine d'Arcachon, 2, rue du Professeur Jolyet, F-33120 Arcachon, France.

* Corresponding author.
E-mail address: d_morse@lifesci.lscf.ucsb.edu (D.E. Morse).

1074-5521/01/$ – see front matter
PII: S1074-5521(01)00072-2

ical silicification (diatoms and sponge spicules) [2–5]. Understanding those mechanisms leads to bioinspired approaches in materials science and may provide a key for environmentally benign routes to manufacture silica-based materials and novel complex materials with naive organic compounds [6–8].

Diatoms take up dissolved Si as undissociated silicic acid, $Si(OH)_4$, [9] from their surrounding aqueous environment where $Si(OH)_4$ concentrations are usually found at the micromolar level ($\leq$80 μM and typically $<$10 μM in the ocean). Physiological studies have shown that transmembrane silicic acid transport in diatoms is regulated by an active transport system [10–12], Na^+-dependent and selective for Si [13–15]. Once incorporated, Si is transported into a membrane-bounded organelle called the Si deposition vesicle (SDV) where daughter cell frustules are synthesized [16–18]. After Si-transportation into the cell, diatoms can maintain intracellular pools of unpolymerized soluble Si ranging from 1 to 27% of the total Si content [19–21]. Recent estimates and measurements have shown that intracellular concentrations can reach 340 mM, and up to 2 M in the species *Ditylum brightwellii* [21,22]. However, in aqueous solution, the threshold concentration for spontaneous formation of colloidal or polymeric Si is only $\sim$2 mM [23], at pH $<$ 10. At higher concentrations, monosilicic acid polymerizes by dehydration to polysilicic acid, forming colloidal silica (silica sol) and then silica gel in supersaturated solutions [24,25]. It has been hypothesized that uncontrolled Si polymerization within the cell might be prevented by interaction of Si with organic molecules (such as ionophores [26]), or by the possible sequestration of Si into Si transport vesicles (STVs), but these possibilities are largely unproven [27].

The recent isolation and characterization of molecules have revealed some transport mechanisms involved in silicification. New families of proteins and genes involved in biosilicification have recently been identified from diatoms [5,15,28–30] and sponges [2]. Various studies have focused on morphogenesis and frustule formation (reviewed in [31–33]) and on Si biomineralization processes [19,34,35]. However, the intracellular forms of Si and the molecular/biochemical pathways involved in silicification are still not elucidated.

It has been hypothesized that Si deposition occurs under acidic conditions inside the SDV [33], and recently Vrieling et al. [4] showed evidence of acidity inside the SDV by observing the accumulation of an acidotropic agent in this structure. Furthermore, polycationic peptides (silaffins) isolated from diatom frustules have been shown to direct formation of silica particles in vitro with their maximal activity at pH 5 [5].

In recent years, studies of molecular/cellular dynamics of inorganic compounds have progressed dramatically owing to the development of appropriate fluorescent probes (fura-2 for Ca^{2+} imaging, carboxyfluorescein for H^+, e.g. [36]), in conjunction with that of modern techniques in microscopy and electronic imaging. For Si, rhodamine 123 has previously been used [37,38] but its low accumulation efficiency relative to the bright autofluorescence of the cells (due to pigments) requires diatom cell washing and fixation prior to fluorescence observation. Bis(cyclopentadienyl)titanium dichloride was also reported as a staining agent for biological silica [39], but this compound is insoluble in aqueous solution and therefore not applicable for living specimens. Hodson et al. [55] labeled plant silica fibers with fluorescein through the silane coupling agent, 3-aminopropyl triethoxysilane, to study the interactions of the mammalian cells with the silica fibers which may cause lung, skin and esophageal cancer. This method, however, can be applied only for post-staining of silica exposed on the surface of materials.

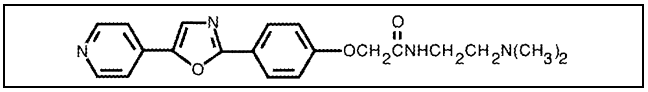

Fig. 1. Chemical structure of PDMPO [41].

In this study, we describe a new application for a known fluorescent pH indicator, the 2-(4-pyridyl)-5-((4-(2-dimethylaminoethylaminocarbamoyl)methoxy)phenyl)oxazole (PDMPO, Fig. 1) (LysoSensor™ DND-160 yellow/blue from Molecular Probes, Eugene, OR, USA) [40,41]. We show that PDMPO quickly enters diatom cells and is specifically incorporated into the newly synthesized frustules, and can therefore been used as an ideal fluorescent tracer for Si. PDMPO possesses unique fluorescent properties in the presence of polysilicic acid showing a bright green fluorescence. In this paper, we present the characterization of the fluorescent properties of PDMPO in relation with Si, and the first results obtained as a biosilicification tracer in living cells.

2. Results

2.1. *Effect of pH and silicic acid on the spectral properties of PDMPO*

The absorption spectra of PDMPO at pH 3.0–7.0 are shown in Fig. 2a,b, in the absence (Fig. 2a) or in the presence (Fig. 2b) of 100 mM silicic acid. In accordance with Diwu et al. [41] PDMPO shows a single absorption peak at 380 nm at pH 3.0 without added silicic acid. The spectrum is shifted to shorter wavelengths with increasing pH, showing a single peak at 338 nm above pH 4.0. In the presence of silicic acid, the absorption spectra of PDMPO and the position of the peaks from pH 3.0 to 7.0 are not significantly changed.

Using the maximum absorption wavelengths obtained above as the excitation wavelengths, the emission fluorescence spectra of PDMPO were measured from pH 3.0 to 7.0 (Fig. 2c,d). At pH 3.0, the fluorophore shows a single

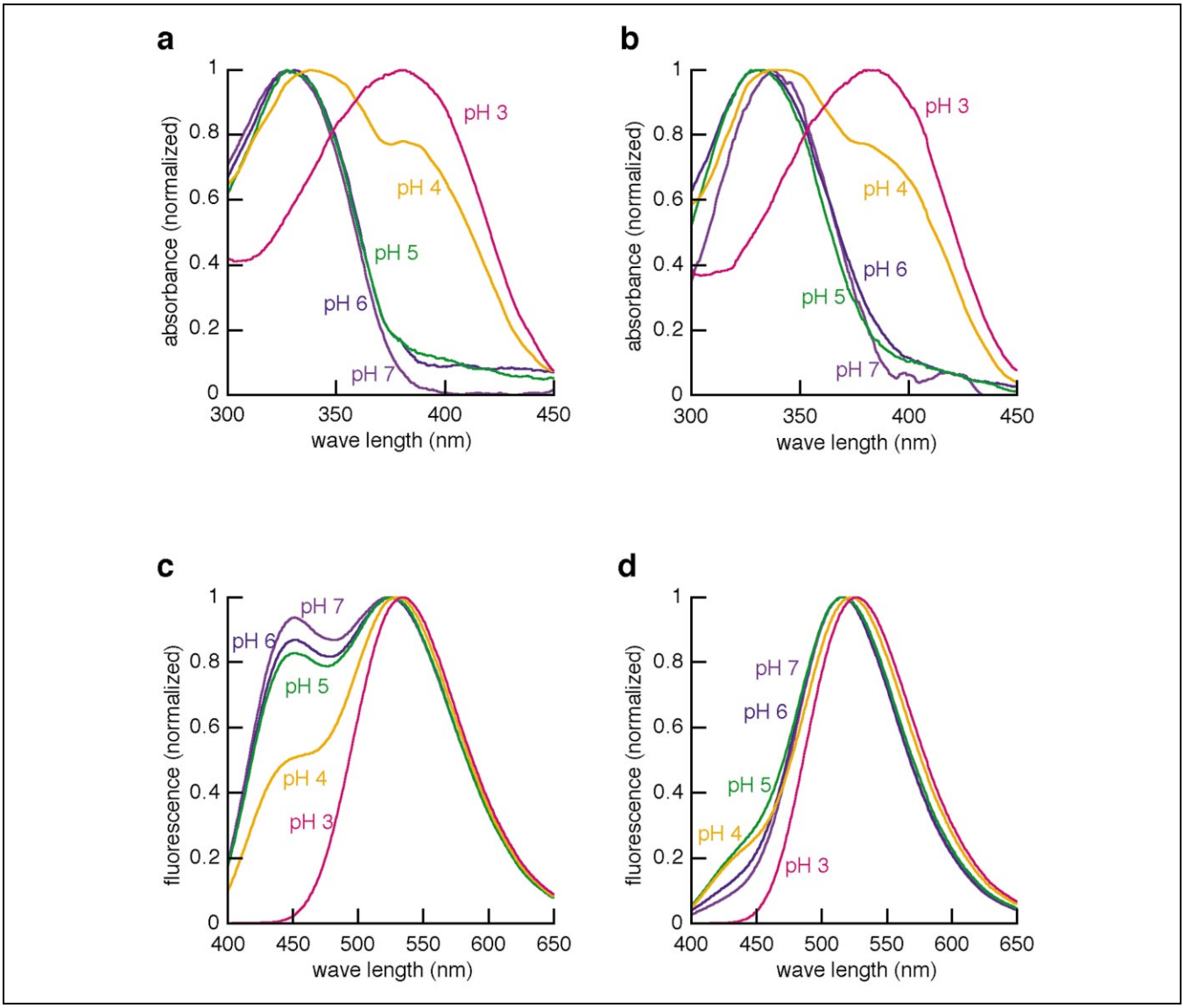

Fig. 2. pH- and Si-dependent spectral response of PDMPO. (a) Normalized absorption spectra of PDMPO alone; (b) normalized absorption spectra of PDMPO in the presence of silicic acid; (c) normalized fluorescence emission spectra of PDMPO alone; (d) normalized fluorescence emission spectra of PDMPO in the presence of silicic acid.

peak at 534 nm. A pH increase results in a slight shift of this peak toward 525 nm at pH 5.0–7.0 with the additional occurrence of first a shoulder and finally a distinctive second peak at 450 nm. The intensity of this 450 nm peak increases with pH, resulting in two distinct emission peaks at 450 nm and 525 nm in the pH range from 5.0 to 7.0 (Fig. 2c). In the presence of 100 mM silicic acid (Fig. 2d), the spectra are blue-shifted and a single peak occurs across the entire pH range tested (pH 3–7); it occurs at 527 nm at pH 3.0, and is shifted toward 510 nm at higher pH. Interestingly, the fluorescence quantum yield of PDMPO in the presence of silicic acid was 1.12 ($\pm$0.05) times greater than that without silicic acid.

The fluorescence spectra of PDMPO at various pH values were also recorded in the presence of silica gel showing similar characteristics (data not shown).

2.2. *Range of Si concentrations modifying the fluorescence emission of PDMPO*

The emission fluorescence of PDMPO (338 nm ex.) at pH 7.0 and various silicic acid concentrations was determined by ratiometric measurement of emission intensities at 510 nm and at 450 nm corresponding to the emission peaks observed with and without added Si respectively (Fig. 3). The 510/450 nm ratio increases with silicic acid concentrations and seems to reach a plateau above $\sim$80 mM (Fig. 3a), probably due to the disappearance of the

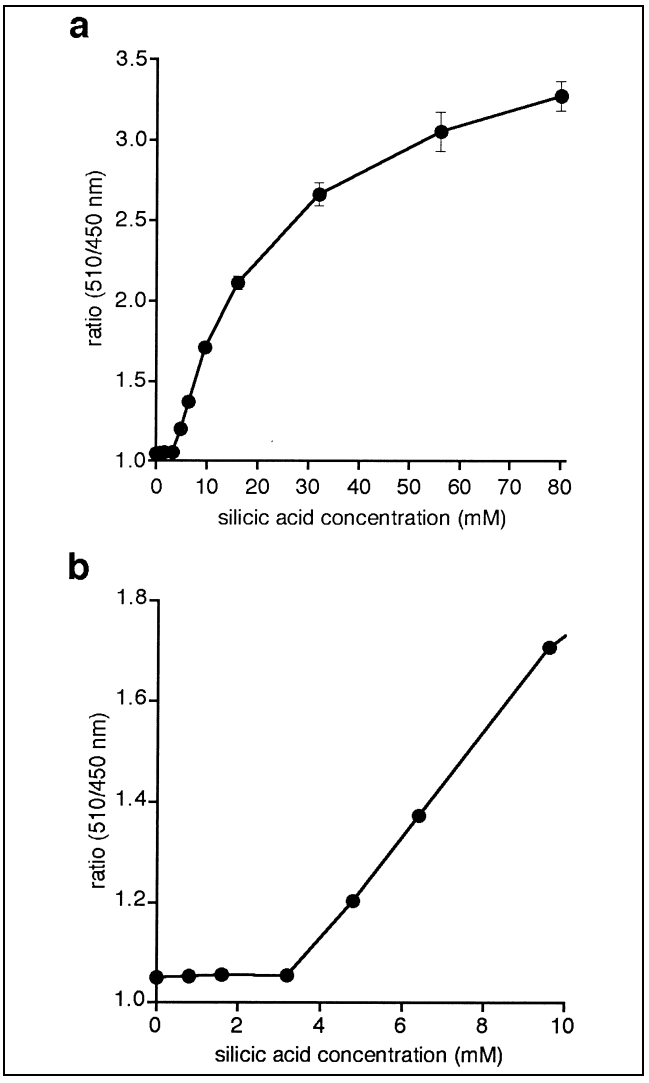

Fig. 3. Effect of silicic acid concentrations (0, 0.8, 1.6, 3.2, 4.8, 6.4, 9.6, 16, 32, 56 and 80 mM Si) on the fluorescence emission of PDMPO. The 510 to 450 nm emission ratio is plotted (338 nm ex.). (a) Emission ratio in the presence of 0 to 80 mM silicic acid; (b) Emission ratio in the presence of <10 mM silicic acid. Circles and bars represent averages of three independent measurements and their respective standard deviations.

450 nm peak. However, silicic acid concentrations <3.2 mM do not significantly affect the fluorescence properties of PDMPO (Fig. 3b).

2.3. *Dynamics of Si polymerization monitored by PDMPO fluorescence*

Changes in the fluorescence intensity (338 nm ex./510 nm em.) of PDMPO were determined as a function of time after addition of 100 mM silicic acid to the PDMPO buffered solution (pH 7.0) (Fig. 4). Simultaneously, the concentration of molybdate-reactive Si was monitored through time as a proxy for Si polymerization as only monomers and dimers of silicic acid are measured by the molybdate method. In the absence of silicic acid, constant

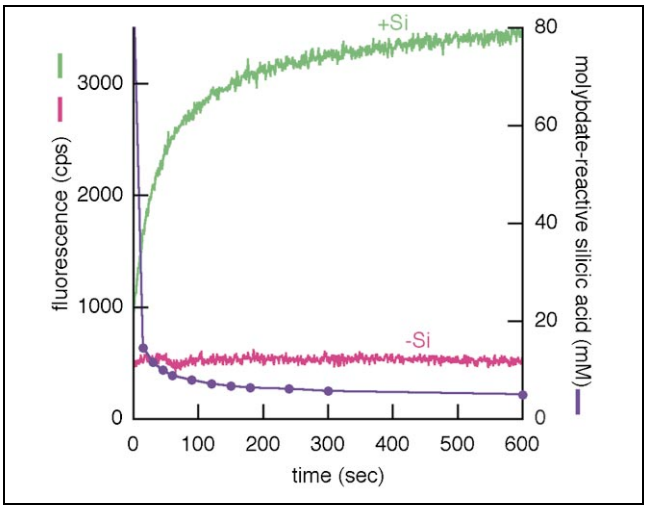

Fig. 4. Effect of Si polymerization on the fluorescence emission intensity of PDMPO at 510 nm (338 nm ex.). The fluorescence intensity in the presence (green) and absence (red) of silicic acid were recorded at 1 s intervals. The concentration of molybdate-reactive silicic acid in solution is shown.

fluorescence intensity was observed during the duration of the experiment. After addition of silicic acid, the fluorescence intensity rapidly increases in the first 60 s, reaching a seven times greater fluorescence after 10 min. Simultaneously to this emission intensity increase, concentrations of molybdate-reactive Si in solution drop, indicating Si polymerization. Silicic acid decreased from 88 mM to 15 mM during the first 15 s, and reached 5 mM after 10 min.

The concentrations of molybdate-reactive Si were also monitored through time in the absence of PDMPO and show the same pattern, suggesting that polymerization of Si with time was not in any way caused nor altered by the presence of PDMPO (data not shown).

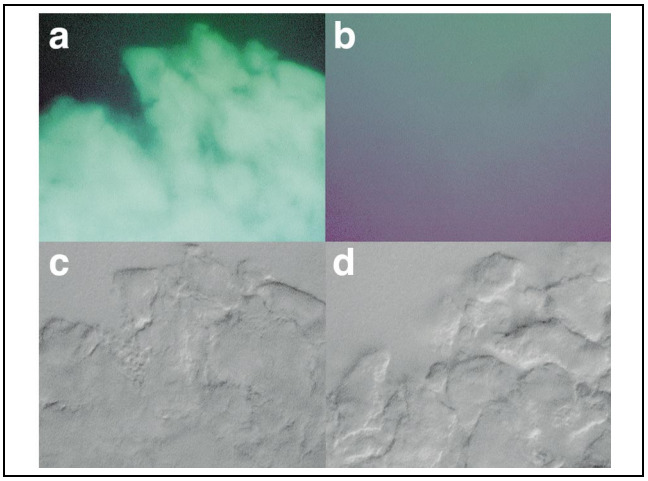

Fig. 5. Fluorescence microphotographs of silica gel in the presence of PDMPO. (a) Fluorescence image of silica gel mixed with PDMPO; (b) fluorescence image of silica gel alone; (c,d) differential interference contrast (DIC) images of the same fields as (a) and (b), respectively.

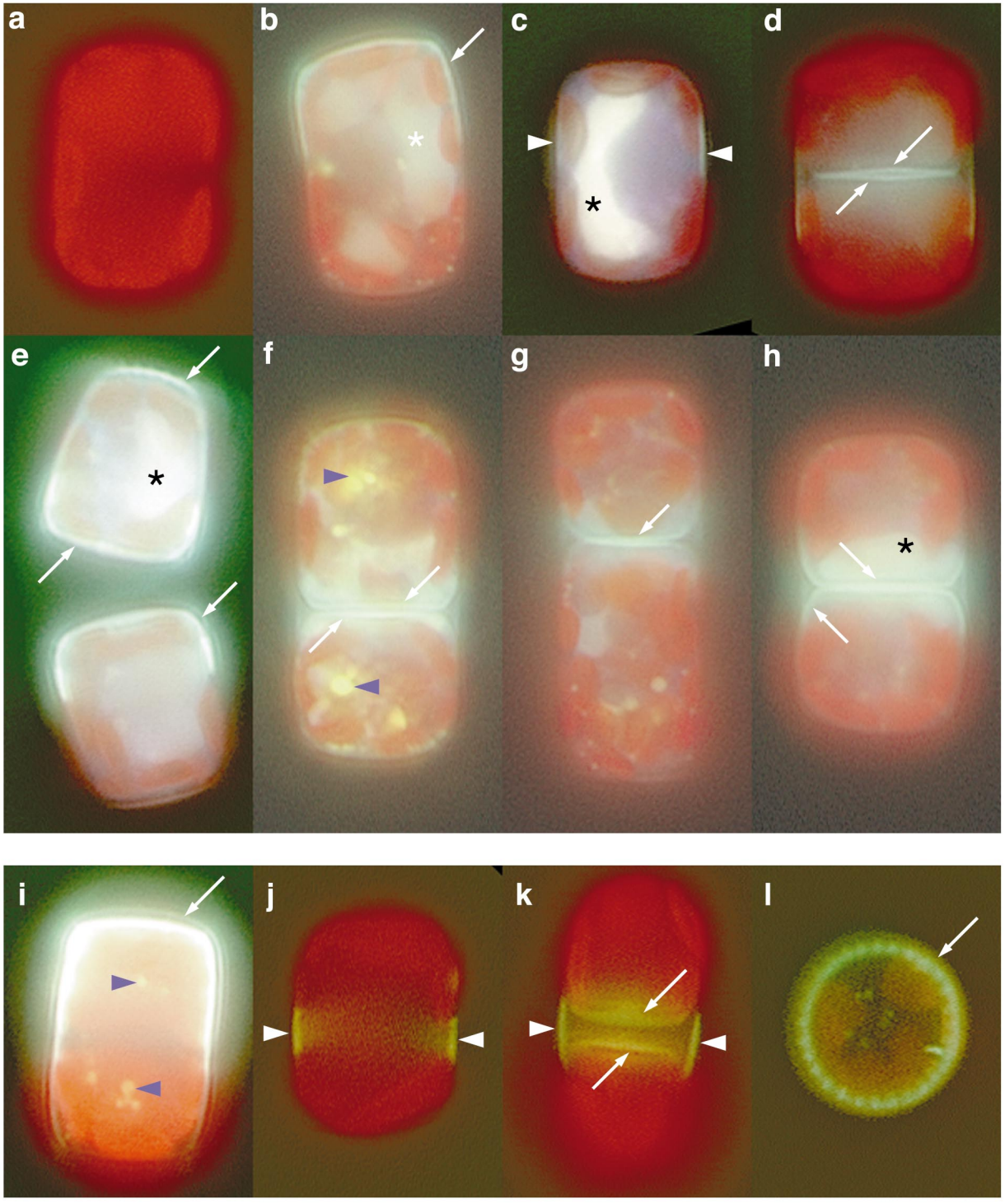

Fig. 6. Fluorescence microphotographs of living diatom cells of *T. weissflogii*. (a) Cells cultured without PDMPO; (b–h) cells (different individuals) grown in the presence of PDMPO; (i–l) cells grown with PDMPO were treated with 10 μM monensin and 10 μM nigericin. Asterisks show fluorescent areas in the intracellular region. Arrows indicate valves; white arrowheads, fluorescence in girdle bands; gray arrowheads, yellow vesicles.

2.4. Imaging of PDMPO fluorescence in the presence of silica gel

The fluorescence of PDMPO in silica gel buffered from pH 3.0 to 7.0 was observed under the fluorescence microscope. Fig. 5 shows results at pH 7.0 and similar results were obtained at other pHs. The silica gel shows an intense green fluorescence when PDMPO is added (Fig. 5a), while no fluorescence was observed without the fluorophore (Fig. 5b).

2.5. Imaging of PDMPO fluorescence in diatom cells

The diatom *Thalassiosira weissflogii* was cultured in the presence of PDMPO and the emission fluorescence was observed using a fluorescence microscope (Fig. 6). Fig. 6a shows the bright red autofluorescence of the chloroplasts in live cells before the addition of PDMPO. When cultured in the presence of PDMPO, the cells rapidly (<5 min) show a very intense yellow/green – almost white – fluorescence in wide portions of the intracellular region. Those fluorescent areas (asterisks in Fig. 6b,c,e,h) were often difficult to image due to the fast bleaching/fading occurring after a few seconds of UV-light exposure. At some occasions, some small bright yellow vesicles are visible in the cell (blue arrowheads in Fig. 6f). In some cells and after less than 1 h, some areas of the frustules start showing an intense green fluorescence (Fig. 6b–h), allowing clear visualization of the areas of the frustule that were newly deposited during the incubation with PDMPO. The fluorescent areas of the frustules as well as the number of stained cells increase as a function of culture duration, and within short incubation times it is possible to observe deposition of new valves (Fig. 6b,d,e,f,g,h) and girdle bands (Fig. 6c).

Treatment of the stained cells with 10 μM solution monensin and nigericin ionophores caused the disappearance of the intracellular fluorescent regions (Fig. 6i–l). However, this allowed the easier observation of the fluorescent frustules as well as the bright yellow vesicles (blue arrowheads in Fig. 6i).

Cells that had incorporated PDMPO into portions of their frustules were cleaned of organic material and were observed under the fluorescence microscope (Fig. 7). The cleaned frustules, both valves (Fig. 7a) and girdle bands (Fig. 7b), showed uniform intense green fluorescence, indicating that the fluorophore has been incorporated into the newly synthesized silica. For comparison, the large

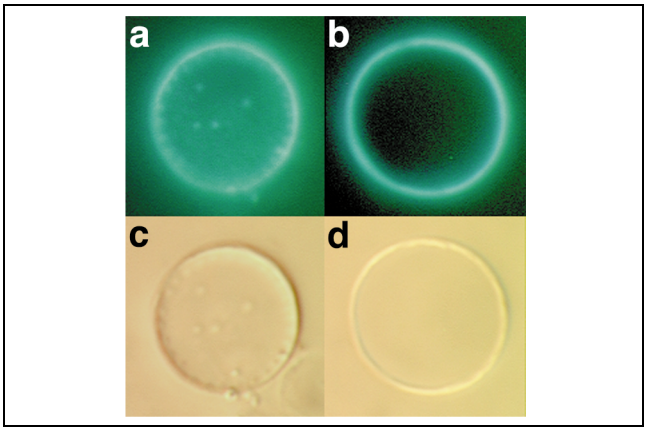

Fig. 7. Fluorescence microphotographs of diatom frustules. Diatoms cultured with PDMPO were treated with oxidizing agents to isolate organic-free frustules. (a) Fluorescence image of a valve; (b) a girdle band; (c,d) DIC images of the same fields as (a) and (b), respectively.

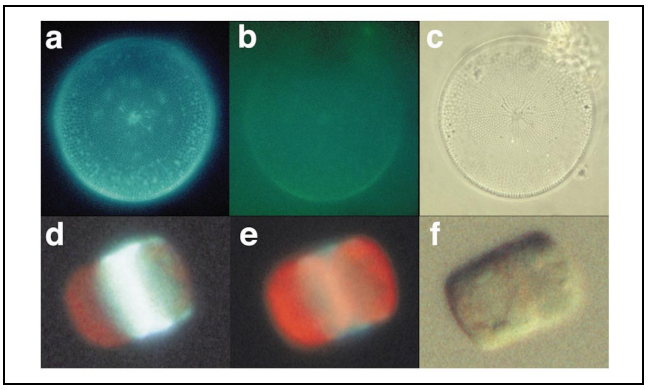

Fig. 8. Fluorescence microphotographs of cleaned valves of the diatom *C. wailesii*, and living cells of *T. weissflogii* after 24 h incubation with rhodamine 123 and PDMPO. (a–c) *C. wailesii*; (d–f) *T. weissflogii*. (a,d), PDMPO; (b,e) rhodamine 123; (c,f) DIC images.

diatom *Coscinodiscus wailesii* was cultured in the presence of PDMPO and of rhodamine 123. Fig. 8 shows the cleaned valves of the cells after 24 h incubation with the dyes, clearly demonstrating the more intense fluorescent staining with PDMPO (Fig. 8a,d) than with rhodamine 123 (Fig. 8b,e).

The emission fluorescence of the PDMPO-stained and cleaned frustules of *T. weissflogii* (ca. 2 μmol biogenic Si suspended in 10 ml of pH 8 buffer) was measured at 338 nm, and showed an intense single peak at 484 nm (data not shown).

3. Discussion

3.1. Modification of the fluorescence properties of PDMPO by Si

As shown by Diwu et al. [41], PDMPO is a fluorophore that exhibits both dual-excitation and dual-emission spectral peaks that are pH-dependent (Fig. 2). In acidic organelles ($pH<5$) the fluorescence is predominantly yellow, while at higher pH ($pH>6$) it has a blue fluorescence [41]. The low p*K*a (4.2) and the changes in excitation and emission wavelengths with pH allow its use as an intracellular pH indicator by emission ratio measurement.

In the case of our experiments pH determination was not possible by color of fluorescence. It is known that solution environment can modify the fluorescence properties of some fluorophores. Diwu et al. [41] observed that the fluorescence of PDMPO is relatively insensitive to ionic strength in aqueous solutions (in either the presence or absence of 100 mM NaCl or KCl), as well as to other halogen ions (Br^- or I^-) and to cationic ions (Mg^{2+} and Ca^{2+}). In this study, we observed that the presence of 100 mM silicic acid solution has significant effects both on the emission wavelengths and on the emission intensity. Si caused a significant shift of the emission fluorescence resulting in a single 510-nm peak at any pH above 3, i.e.

spectra similar to those found in acidic solutions, confounding the determination of pH in the presence of Si.

The silicic acid concentration threshold for the formation of colloidal or polymeric Si is about 2 mM at pH < 10 [23,24]. In supersaturated solutions and neutral pH, monomeric silicic acid spontaneously polymerizes into oligo- and polymeric silicic acid, silica sol, and finally silica gel [25]. When the 100 mM silicic acid solution is added to PDMPO, the increase of the emission fluorescence intensity at 510 nm is clearly observed simultaneously with the decrease of the molybdate-reactive silicic acid in solution (monomeric or oligomeric silicic acid) (Fig. 4). The fluorescence intensity increase is slightly slower than the Si polymerization process, suggesting that the fluorescence shift is due to the presence of polymeric forms of silicic acid. This also is supported by the fact that the emission fluorescence spectra is not shifted with silicic acid concentrations < 3.2 mM (Fig. 3).

In addition, the presence of silicic acid results in a noteworthy increase in the fluorescence intensity of PDMPO at 510 nm (Fig. 4), suggesting some 'silica-philic' properties of PDMPO. Hence, the significant effects of Si both on the emission wavelengths and on the emission intensity make this compound an excellent new probe for imaging polysilicic acid and silica in a wide range of biological and chemical studies.

3.2. Tracing frustule silicification in diatom cell cultures

In recent years, fluorescent pH indicators have widely been developed [42] to monitor intracellular pH changes. However, most of the dyes commonly used for this purpose were little adapted to study acidic organelles because they do not selectively accumulate in acidic compartments or because their fluorescence is greatly reduced in acidic media [36,43–48]. Recently, Vrieling et al. [4] suggested an acidic environment inside the SDV of pennate diatoms *Navicula* spp. by showing the accumulation of an acidotropic, non-fluorescent probe (DAMP), which they localized with specific antibodies. In their study, they also used several pH-sensitive fluorescent probes to determine the compartmental pH but fluorescence ratio analysis was not possible due either to the lack of specific accumulation of the dyes into the SDV or due to the lack of sensitivity of the fluorophores. PDMPO is an acidotropic probe with a low p*K*a that has been shown to accumulate in acidic organelles [41]. The novelty of this probe is that it shows a fast accumulation into the SDV where silica is deposited into the new frustules. This feature is also observed with the fluorophore rhodamine 123. In previous studies [4,37] rhodamine 123 has been used to label and visualize the newly formed siliceous cell walls of fixed diatom cells by fluorescence microscopy. Fixation and rinsing of the samples are necessary with rhodamine 123 because of the low emission intensity of rhodamine 123 relative to the bright red autofluorescence of the cells, and because of the high concentration of the dye in the growth medium necessary to stain the cells. Brzezinski and Conley [38] used rhodamine 123 in order to quantify the amount of Si deposited during each stage of the diatom cell cycle by using flow cytometry and quantitative measurements of the incorporated dye. However, they disregarded the use of microscopy for this dye due to its limits for the visualization of specific frustule elements in *T. weissflogii* as described in Fryxell et al. [49].

Hence, as for rhodamine 123, PDMPO is trapped within the solid silica matrix of the frustule, but because of its intense fluorescence, PDMPO can be visualized either in living or fixed cells. In this study, we show that PDMPO can be applied to the visualization on a fluorescent microscope of live cells, and therefore to observe the timing of the intracellular Si polymerization (polysilicic acid) and deposition into the SDV (silica), without complex sample preparations. The observation of frustule formation is possible throughout the different steps of the cell cycle with sequential staining of single elements such as the central valve region (Fig. 6d,f,g,h), the whole epi- and/or hypovalves (Fig. 6b,e,i), the girdle bands (Fig. 6c,j,k), and some details of the fine structure of the frustules such as striae and processes (Fig. 6e,l). The possibility to visualize such frustule microstructures may be used for taxonomic purposes with effortless sample preparation.

Control experiments with ionophores suggest that the bright green/blue fluorescence observed in wide portions of the intracellular region might be due to higher pHs (cytosol, nucleus, mitochondria, or other microbodies). Interestingly, the small bright yellow vesicles remain after addition of the ionophores (Fig. 6f,i), suggesting a PDMPO–silica (or polysilicic acid) interaction and may be revealing STVs. Schmid and Schulz [29] have suggested the existence of such cytoplasmic vesicles, however, these have not clearly shown any Si content, and their role is still uncertain.

3.3. Mechanisms of incorporation and co-deposition of PDMPO with Si in diatoms

PDMPO and rhodamine 123 quickly enter the cells due to their membrane-permeable properties. They both show a fast accumulation into the SDV where silica is deposited into the new frustules and they are both trapped within the solid silica matrix of the frustule. It is conceivable that the mechanisms involved in the incorporation of those fluorophores are similar. They both are co-deposited with Si, and stained frustules, cleaned of their organic coating, still show their fluorescence, which can be kept for months in the dark. Furthermore, when incorporated simultaneously, their fluorescent properties do not change (Fig. 8) indicating that they do not interact together.

Li et al. [37] hypothesize that rhodamine 123 accumulation results from a transmembrane potential or a high reducing potential in the SDV, but the exact mechanism of

incorporation is not known [38]. PDMPO is supposed to accumulate into lysosomes and other acidic organelles, therefore suggesting acidity inside the silicalemma as previously hypothesized [4,33]. However, the change of the fluorescent properties of PDMPO with Si might also suggest some previous interaction of the molecule with polymeric silicic acid or silica (by hydrogen or covalent bonds) in the STV or SDV and the subsequent deposition of the new complex into the frustule.

4. Significance

In this study we showed the unique fluorescence properties of PDMPO in the presence of polymeric silicic acid and silica, and its effective application for imaging silicification in living diatom cells.

In addition, this molecule can be relevant for a wide range of applications provided Si polymerization takes place in the presence of PDMPO. In biology, this molecule can be applied for studies on silicification in not only diatoms but also sponges and higher plants. It is obvious that the efficiency of the technique shown on diatoms is of major interest in oceanography and plankton ecology, Si-cycling and primary production in the oceans. Within the clinical research field, one could envisage the use of PDMPO to help explain how asbestos or other silica fibers from grasses cause lung fibrosis and cancer, dermatitis, esophageal cancer, thoracic tumors, to help elucidate the requirement for Si in the formation of the vertebrate skeleton, and evaluate implantation of Si-containing artificial bones. The wide range of industrial applications of silica has encouraged inorganic chemistry and materials science to search for new 'bioinspired' high performance composite materials. The possible use of a new fluorescent Si-tracer can allow straightforward studies of the dynamics of silica chemistry in real time.

5. Materials and methods

5.1. Fluorescent dyes

PDMPO (1 mM in dimethylsulfoxide) was obtained from Molecular Probes (LysoSensor™ yellow/blue DND-160, Fig. 1). Rhodamine 123 was obtained from Sigma.

5.2. Absorption and fluorescence spectra of PDMPO

PDMPO was dissolved at a concentration of 20 μM in 0.1 M Na-phosphate buffer (pH 3.0, 4.0, 5.0, 6.0 and 7.0). For experiments in the presence of silicic acid, a 100 mM silicic acid solution was prepared by passing a 0.5 M Na_2SiO_3 solution through a cation-exchange resin Rexyn 101(H) (Fisher Scientific, PA, USA). The absorption spectra of PDMPO in buffer solution with or without silicic acid were recorded on a spectrophotometer DU-7, Beckman (CA, USA), and the emission fluorescence spectra were recorded on a FluoroMax-2 spectrofluorometer (Instruments SA, NJ, USA) using the excitation wavelength where maximum absorption was obtained. The relative fluorescence quantum yield of PDMPO in the presence of silicic acid was determined by comparison to that of PDMPO alone according to Diwu et al. [41].

5.3. Effect of silicic acid concentration on the fluorescence properties of PDMPO

A series of solutions of 1 μM PDMPO in 0.1 M Na-phosphate buffer (pH 7.0) was prepared with different silicic acid concentrations ranging from 0 to 80 mM. The fluorescence of each solution was then measured at 450 and 510 nm with an excitation wavelength of 338 nm, and the ratios of those two emission fluorescence intensities were calculated.

5.4. Effect of Si polymerization on the fluorescence properties of PDMPO

Two silicic acid solutions prepared as above were added to buffer solutions with or without PDMPO (100 mM silicic acid, 0.1 M Na-phosphate buffer pH 7.0, 1 μM PDMPO final concentrations). The fluorescence intensities of solutions with or without PDMPO (338 nm ex.; 510 nm em.) were recorded at 1 s and 1 min intervals, respectively. Aliquots of each solution were subsampled at a 15 s interval for determination of molybdate-reactive silicic acid concentrations to monitor Si polymerization (according to Strickland and Parsons [50]).

5.5. PDMPO fluorescence in silica gel

A silica gel of 5 mg/ml final concentration (Aldrich) was prepared with 0.1 M Na-phosphate buffer at pH 3.0, 4.0, 5.0, 6.0 and 7.0, either in the presence or absence of 1 μM PDMPO. Each gel was laid over a glass slide and observed under a fluorescence microscope (Olympus BX-60) equipped with a real-time enhancement digital video camera (Optronics LE-Digital), and fitted with a wide-band cube Olympus U-MWU filter (UV ex. light 330–385 nm; transmission $>$ 420 nm).

5.6. PDMPO fluorescence in diatom cell cultures

Two different diatom species were tested in our experiments. *C. wailesii* Gran and Angst was chosen because of its large cell size (360–380 μm) and *T. weissflogii* (Grunow) G. Fryxell and Hasle was used because of its large internal pools of dissolved Si. Binder and Chisholm [51] observed that internal pools can represent up to 35% of total cellular Si in this diatom when Si-starved cells were presented with a pulse of Si and that those pools can be sustained for several hours.

The diatom *T. weissflogii* has been maintained in culture at UCSB for several years. The diatom *C. wailesii* (clone GB395G-CCMP 1818) was obtained from the Provasoli-Guillard National Center for Culture of Marine Phytoplankton (CCMP) at the Bigelow Marine Laboratory for Ocean Sciences (ME, USA). Cells were cultured in f/2 enriched seawater medium with added dissolved Si [52,53] at 17°C under a continuous photon fluence rate of approximately 100 μmol photon/m^2 s.

For the purpose of the experiments, 250 ml of dense ($\sim$400 000 cell/ml of *T. weissflogii* or 50 000 cell/ml of *C. wailesii*) Si-starved cultures were incubated in the presence of PDMPO and silicic acid to allow cell growth and Si incorporation. Si was added to

a final concentration of 400 μM and the 1 mM PDMPO stock solution was diluted to a final working concentration in the growth medium for all diatom experiments. The concentration of PDMPO for optimal staining may vary depending on concentrations of both dissolved Si and diatom cells as well as on the length of incubation. Here we used 1 μM PDMPO which appeared appropriate for our culture conditions, e.g. at this concentration, growth rates were unaffected and optimal staining of the frustules was obtained. The cells were incubated under appropriate growth conditions for at least 1 day and observed at regular intervals.

At different stages during the PDMPO incubation, 10 μM solutions of the ionophores monensin and nigericin were added to sub-samples of the stained *T. weissflogii* diatoms and incubated for 2 min to release any unbound PDMPO molecules from the cells. Similar incubations of *T. weissflogii* cells were performed by using rhodamine 123 diluted to a final concentration of 2 μg. ml^{-1} in the growth medium.

After 3 days of incubation with PDMPO or rhodamine 123, stained cells were cleaned following the procedure of Simonsen [54]. Briefly, the cells were treated in saturated $KMnO_4$ solution for 1 h and then heated up to 80°C with equal volume of concentrated HCl. The remaining material was rinsed several times with Milli-Q water until neutral conditions ($pH > 5$) were approached.

Live cells and cleaned frustules were observed on a glass slide using the previously described fluorescence microscope and digital camera. Only live cells stained with rhodamine 123 needed further rinses before microscopic examination due to the high fluorescent background in the medium. In addition, the emission fluorescence spectrum of the cleaned frustules of PDMPO-stained cells of *T. weissflogii* was recorded with an excitation wavelength of 338 nm.

Acknowledgements

We thank B. Matsumoto for technical assistance and helpful discussions. This work was supported by Grants from the US Army Research Office Multidisciplinary University Research Initiative (DAAH04-96-1-0443), the US Office of Naval Research (N00014-93-1-0584), the Materials Research Division of the National Science Foundation (MCB-9202775), the NOAA National Sea Grant College Program, US Department of Commerce, under Grant NA36RG0537, Project E/G-2, through the California Sea Grant College System, the MRSEC Program of the National Science Foundation under Award no. DMR-96-32716 to the UCSB Materials Research Laboratory, and donation from the Dow Corning Corporation Genencor International Inc. The US Government is authorized to reproduce and distribute copies for governmental purposes.

References

[1] E. Epstein, The anomaly of silicon in plant biology, Proc. Natl. Acad. Sci. USA 91 (1994) 11–17.

[2] K. Shimizu, J. Cha, G.D. Stucky, D.E. Morse, Silicatein α: cathepsin L-like protein in sponge biosilica, Proc. Natl. Acad. Sci. USA 95 (1998) 6234–6238.

[3] W.H. van de Poll, E.G. Vrieling, W.W.C. Gieskes, Location and expression of frustulins in the pennate diatoms *Cylindrotheca fusiformis*, *Navicula pelliculosa*, and *Navicula salinarum* (Bacillariophyceae), J. Phycol. 35 (1999) 1044–1053.

[4] E.G. Vrieling, W.W.C. Gieskes, T.P.M. Beelen, Silicon deposition in diatoms: control by the pH inside the silicon deposition vesicle, J. Phycol. 35 (1999) 548–559.

[5] N. Kröger, R. Deutxmann, M. Sumper, Polycationic peptides from diatom biosilica that direct silica nanosphere formation, Science 286 (1999) 1129–1132.

[6] E.G. Vrieling, T.P.M. Beelen, R.A. van Santen, W.W.C. Gieskes, Diatom silicon biomineralization as an inspirational source of new approaches to silica production, J. Biotechnol. 70 (1999) 39–51.

[7] D.E. Morse, Silicon biotechnology: harnessing biological silica production to construct new materials, Trend. Biotechnol. 17 (1999) 230–232.

[8] K. Shimizu, D.E. Morse, Biological and biomimetic synthesis of silica and other polysiloxanes, in: E. Bauerlein (Ed.), Biomineralization, Wiley-VCH, Weinheim, in press.

[9] Y. Del Amo, M.A. Brzezinski, The chemical form of dissolved Si taken up by marine diatoms, J. Phycol. 35 (1999) 1162–1170.

[10] F. Azam, B.B. Hemmingsen, B.E. Volcani, Role of silicon in diatom metabolism. V. Silicic acid transport and metabolism in the heterotrophic diatom *Nitzschia alba*, Arch. Microbiol. 97 (1974) 103–114.

[11] F. Azam, B.E. Volcani, Germanium–silicon interactions in biological systems, in: T.L. Simpson, B.E. Volcani (Eds.), Silicon and Siliceous Structures in Biological Systems, Springer-Verlag, New York, 1981, pp. 43–68.

[12] D. Werner, Silicate metabolism, in: D. Werner (Ed.), The Biology of Diatoms, University of California Press, Berkley, CA, 1977, pp. 110–149.

[13] C.W. Sullivan, Diatom mineralization of silicic acid. II. Regulation of $Si(OH)_4$ transport rates during the cell cycle of *Navicula Pelliculosa*, J. Phycol. 13 (1977) 86–91.

[14] P. Bhattacharyya, B.E. Volcani, Sodium-dependent silicate transport in the apochlorotic marine diatom *Nitzschia alba*, Proc. Natl. Acad. Sci. USA 77 (1980) 6386–6390.

[15] M. Hildebrand, B.E. Volcani, W. Gassmann, J.I. Schroeder, A gene family of silicon transporters, Nature 385 (1997) 688–689.

[16] R.W. Drum, H.S. Pankratz, Post mitotic fine structure of *Gomphonema parvulum*, J. Ultrastruct. Res. 10 (1964) 217–233.

[17] B.E.F. Reimann, J.C. Lewin, B.E. Volcani, Studies on the biochemistry and fine structure of silica shell formation in diatoms. II. The structure of the cell wall of *Navicula pelliculosa* (Breb.) Hilse, J. Phycol. 2 (1966) 74–84.

[18] A.M. Schmid, M.A. Borowitzka, B.E. Volcani, Morphogenesis and biochemistry of diatom cell wall, in: O. Kiermayer (Ed.), Cyclomorphogenesis in plants, Cell. Biol. Monogr. 8, 1981, pp. 63–97.

[19] C.W. Sullivan, B.E. Volcani, Silicon in the cellular metabolism of diatoms, in: T.L. Simpson, B.E. Volcani (Eds.), Silicon and Siliceous Structures in Biological Systems, Springer-Verlag, New York, 1981, pp. 15–42,.

[20] M.A. Brzezinski, R.J. Olson, S.W. Chisholm, Silicon availability and cell-cycle progression in marine diatoms, Mar. Ecol. Prog. Ser. 67 (1990) 83–96.

[21] M. Hildebrand, personal communication.

[22] S.W. Chisholm, F. Azam, R.W. Eppley, Silicic acid incorporation in marine diatoms on light:dark cycles: use as an essay for phased cell division, Limnol. Oceanogr. 23 (1978) 518–529.

[23] W. Stumm, J.J. Morgan, Aquatic chemistry: Chemical equilibria and rates in natural waters, Wiley, J. and sons, New York, 1996.

[24] R.K. Iler, The Chemistry of Silica: Solubility, Polymerization, Colloid and Surface Property and Biochemistry, Wiley, New York, 1979.

[25] T. Tarutani, Polymerization of silicic acid: a review, Anal. Sci. 5 (1989) 245–252.
[26] P. Bhattacharyya, B.E. Volcani, Isolation of silicate ionophore(s) from the apochlorotic diatom *Nitzschia alba*, Biochem. Biophys. Res. Commun. 114 (1983) 365–372.
[27] A.M. Schmid, D. Schulz, Wall morphogenesis in diatoms: deposition of silica by cytoplasmic vesicles, Protoplasma 100 (1979) 267–288.
[28] N. Kröger, C. Bergsdorf, M. Sumper, A new calcium binding glycoprotein family constitutes a major diatom cell wall component, EMBO J. 13 (1994) 4676–4683.
[29] N. Kröger, C. Bergsdorf, M. Sumper, Frustulins: domain conservation in a protein family associated with diatom cell walls, Eur. J. Biochem. 239 (1996) 259–264.
[30] N. Kröger, M. Sumper, Diatom cell wall proteins and the cell biology of silica biomineralization, Protist 149 (1998) 213–219.
[31] J. Pickett-Heaps, A.M. Schmid, L.A. Edgar, The cell biology of diatom valve formation, Prog. Phycol. Res. 7 (1990) 1–168.
[32] J. Pickett-Heaps, Cell division in diatoms, Int. Rev. Cytol. 128 (1991) 63–108.
[33] R. Gordon, R.W. Drum, The chemical basis of diatom morphogenesis, Int. Rev. Cytol./A Surv. Cell Biol. 150 (1994) 243–372.
[34] C.W. Sullivan, Silicification by diatoms, in: J. Wiley, (Ed.), Silicon Biochemistry, Ciba foundation Symposium 121, Chichester, 1986, pp. 59–89.
[35] B.E. Volcani, Cell wall formation in diatoms: morphogenesis and biochemistry, in: T.L. Simpson, B.E. Volcani (Eds.), Silicon and Siliceous Structures in Biological Systems, Springer-Verlag, New York, 1981, pp. 157–200.
[36] R.Y. Tsien, Fluorescent indicators of ion concentrations, in: D.L. Taylor (Ed.), Florescence Microscopy of Living Cells in Culture, Vol. 30, Part B, Academic Press, San Diego, CA, 1989, pp. 127–156.
[37] C.-W. Li, S. Chu, M. Lee, Characterizing the silica deposition vesicle of diatoms, Protoplasma 151 (1989) 158–163.
[38] M.A. Brzezinski, D.J. Conley, Silicon deposition during the cell cycle of *Thalassiosira weissflogii* (Bacillariophyceae) determined using dual rhodamine 123 and propidium iodine staining, J. Phycol. 30 (1994) 45–55.
[39] C.C. Perry, E.J. Moss, R.J.P. Williams, A staining agent for biological silica, Proc. R. Soc. Lond. B 241 (1990) 47–50.
[40] S.J. Hurwitz, M. Terashima, N. Mizunuma, C.A. Slapak, Vesicular anthracycline accumulation in doxorubicin-selected U-937 cells: participation of lysozomes, Blood 89 (1997) 3745–3754.
[41] Z. Diwu, C.-S. Chen, C. Zhang, D.H. Klaubert, R.P. Haugland, A novel acidotropic pH indicator and its potential application in labeling acidic organelles of live cells, Chem. Biol. 6 (1999) 411–418.
[42] A.W. Czarnik, Desperately seeking sensors, Chem. Biol. 2 (1995) 423–428.
[43] C.C. Overly, K.D. Lee, E. Berthiaume, P.J. Hollenbeck, Quantitative measurement of intraorganelle pH in the endosomal lysosomal pathway in neurons by using ratiometric imaging with pyranine, Proc. Natl. Acad. Sci. USA 92 (1995) 3156–3160.
[44] V. Sandhu, M. Miller, A.K. Grover, Effects of peroxide on the fluorescence of the Ca^{2+} probe Fluo-3 and the pH probe BCECF, Mol. Cell. Biochem. 178 (1998) 77–80.
[45] J.M. Devoisselle, S. Soulie, S. Mordon, H. Maillols, Fluorescent characteristics and pharmacokinetic profiles of the fluorescent probe BCECF in various tissues: the role of blood content, Photochem. Photobiol. 64 (1996) 906–910.
[46] L.X. Liu, Z.J. Diwu, D.H. Klaubert, Fluorescent molecular probes III. 2′,7′-bis-(3-carboxypropyl)-5-(and-6)-carboxyfluorescein (BCPCF) a new polar dual-excitation and dual-emission pH indicator with a p*K*a of 7.0, Bioorg. Med. Chem. Lett. 7 (1997) 3069–3072.
[47] J.E. Whitaker, R.P. Haugland, F.G. Prendergast, Spectral and photophysical studies of benzo[c]xanthene dyes: dual emission pH sensors, Anal. Biochem. 194 (1991) 330–344.
[48] M. Kneen, J. Farinas, Y. Li, A.S. Verkman, Green fluorescent protein as a noninvasive intracellular pH indicator, Biophys. J. 74 (1998) 1591–1599.
[49] G.A. Fryxell, G.F. Hubbard, T.A. Villareal, The genus *Thalassiosira*: variations of the cingulum, Bacillaria 4 (1981) 41–63.
[50] J.D.H. Strickland, T.R. Parson, A Practical Handbook of Seawater Analysis, Bull. Fish. Res. Bd. Can., Ottawa, 1972.
[51] B.J. Binder, S.W. Chisholm, Changes in the soluble silicon pool size in the marine diatom *Thalassiosira weisflogii*, Mar. Biol. Lett. 1 (1980) 205–212.
[52] R.R.L. Guillard, J.H. Ryther, Studies of marine planktonic diatoms. I. *Cyclotella nana* Hustedt and *Detonula confervacea* Cleve, Can. J. Microbiol. 8 (1962) 229–239.
[53] R.R.L. Guillard, Culture of phytoplankton for feeding marine invertebrates, in: W.L. Smith, M.H. Chanley (Eds.), Culture of Marine Invertebrate Animals, Plenum, New York, 1975, pp. 26–60.
[54] R. Simonsen, in: A. Sournia (Ed.), Phytoplankton Manual, MNHN, Paris, 1974.
[55] M.J. Hodson, R.J. Smith, A. van Blaaderen, T. Crafton, C.H. O'Neill, Detecting plant silica fibres in animal tissue by confocal fluorescence microscopy, Ann. Occup. Hyg. 38 (1994) 149–160.